"SQUASHING THE PEANUT": WHAT IT MEANS FOR *IN-VIVO* CARDIAC DTI

Andrew D Scott[1,2], Sonia Nielles-Vallespin[1,3], Pedro Ferreira[1,2], Laura-Ann McGill[1,2], Dudley Pennell[1,2], and David Firmin[1,2]

[1]*NIHR Cardiovascular Biomedical Research Unit, The Royal Brompton Hospital, London, United Kingdom,* [2]*National Heart and Lung Institute, Imperial College London, London, United Kingdom,* [3]*National Heart, Lung and Blood Institute, National Institutes of Health, Bethesda, Maryland, United States*

Target Audience: Physicists and cardiologists with an interest in myocardial microstructure and diffusion tensor imaging.

Purpose: *In-vivo* cardiac diffusion tensor imaging (cDTI) using stimulated echo acquisition mode – echo planar imaging (STEAM-EPI) sequences[1,2] is often considered a low signal to noise ratio (SNR) technique. The effects of noise at various b-values has been well described in relation to diffusion weighted imaging in the brain[3,4], but the parameters of interest, sequences and tissue studied are quite different in cDTI. In this work, we perform simulations of the effects of noise on parameters derived from cDTI using a cardiac specific simulation framework at a range of b-values. We then demonstrate how the phase of the diffusion-weighted images can be used with the magnitude data to reduce the background noise when multiple averages are used both in simulations and in a cohort of healthy volunteers.

Methods: ***Simulations:*** Based on *in-vivo* data from a previous study[5] simulated maps of helical angle (HA), E2A (absolute angle between the radial direction and the projection of $\hat{e}_2$ into the radial/cross-myocyte plane[6]), mean diffusivity (MD) and fractional anisotropy (FA) were created for a left ventricle-like shape. A simulated diffusion tensor and simulated diffusion weighted images were then calculated for 6 diffusion encoding directions and b-values from 50 – 3000 smm^{-2}. The images were adjusted for simulated T2 related signal loss (T2=50ms) with increasing b-value and, in k-space, zerofilling was simulated and Gaussian noise was added. The simulated data was processed using both the average of the magnitude data and the average of the complex data using the same process used for in-vivo cDTI data. The simulated parameter maps were compared pixel-by-pixel with the input data.

In-vivo imaging: cDTI was performed in one short axis mid-ventricular slice in 10 healthy subjects using a Siemens Skyra 3T scanner with a monopolar STEAM-EPI sequence described elsewhere[2]. Imaging was performed using 6 diffusion-encoding directions (+b0 reference), 2.8x2.8x8mm^3 acquired resolution, 12 averages, SENSE x2 and both the magnitude and phase data was reconstructed. Image phase caused by residual bulk motion between the diffusion encoding gradients was approximated as the phase of a copy of each image multiplied in k-space with a pyramid shaped kernel of width ¼ of the field of view [7,8] and subtracted from the relevant image. These corrected images were then averaged in complex space and parameter maps from this algorithm were compared to those calculated from standard magnitude averaged images.

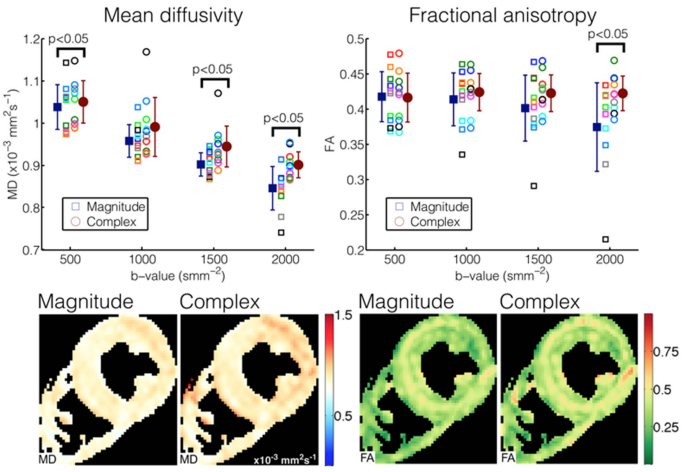

Figure 3: Results showing the mean MD and FA for each subject with magnitude and complex averaging for all acquired b-values (top row). Results where a paired t-test between complex and magnitude results shows a significant difference are marked as such. Example MD (bottom left) and FA maps (bottom right) are also shown for b=2000smm^{-2}.

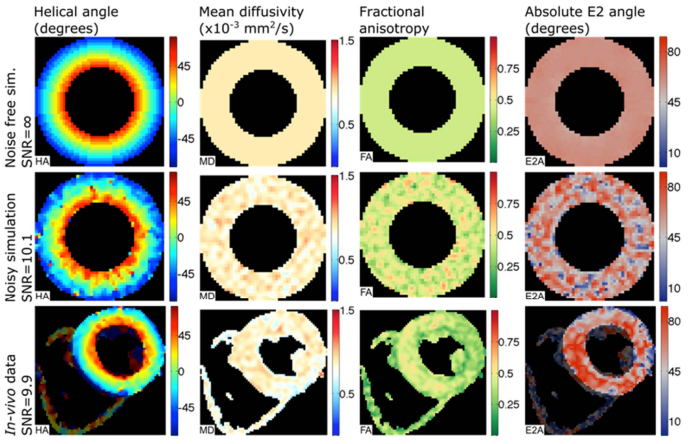

Figure 1: Example parameter maps, showing the simulation input (top row), noisy simulation output (second row, b=700smm-2, 9 averages) and *in-vivo* data with similar SNR (bottom, b=750smm-2, 8 averages).

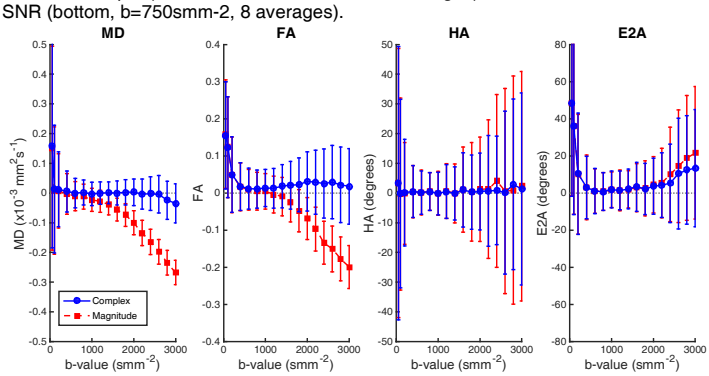

Figure 2: The bias (output measure – input) ± standard deviation plotted with the simulated b-value for magnitude and complex averaging. 11 averages were simulated and noise was adjusted to give an SNR of 16 at b=750smm^{-2}.

Results: Figure 1 compares simulated and in-vivo parameter maps with similar parameters and demonstrates good visual agreement. Figure 2 plots the bias (simulation output – input) ± standard deviation of MD, FA, HA and E2A with b-value for magnitude and complex averaging. MD and FA are over-estimated at low b-values and under-estimated at high b-values when magnitude averaging is used. When complex averaging is used the under-estimation of MD and FA is compensated. Figure 3 shows the results acquired in-vivo. In agreement with the simulations, the reduction in MD and FA with increasing b-values is partially compensated for by complex averaging. The increases in FA and MD are evident in the example MD and FA parameter maps shown (b=2000smm^{-2}).

Discussion: We have developed a framework for performing cardiac specific simulations of the effects of acquisition parameters on cDTI. At low b-values eigenvalue repulsion results in an increase in FA[3] and the practice of replacing negative eigenvalues with positive values from neighbouring pixels inflates MD. The transition from the low b-value regime where MD or FA is over-estimated to the high b-value regime where MD or FA is under-estimated (so-called "squashing the peanut"[4]) occurs at a higher b-value for FA than for MD. Using simulations and data acquired *in vivo*, we have demonstrated that under-estimation of FA and MD in the high b-value regime can be at least partially compensated for by averaging the complex data after accounting for motion-induced phase.

Conclusion: While we did not consider the effects of motion or non-Gaussian diffusion, when cDTI is performed with multiple averages, complex averaging of the data should be considered in combination with relatively high b-values as a method of mitigating the effects of noise on the derived parameters.

References: 1. Reese MRM 1995, DOI: 10.1002/mrm.1910340603
2. Nielles-Vallespin MRM 2012, DOI:10.1002/mrm.24488
3. Basser MRM 2000, DOI: 10.1002/1522-2594(200007)44:1<41::AID-MRM8>3.0.CO;2-O
4. Jones MRM 2004a, DOI:10.1002/mrm.20033
5. Scott MRM 2014, DOI: 10.1002/mrm.25418
6. Ferriera JCMR 2014, DOI:10.1186/s12968-014-0087-8
7. Pipe MRM 2002, DOI:10.1002/mrm.10014
8. Skare ISMRM 2009, 1409